







## Open Archive Toulouse Archive Ouverte (OATAO)

OATAO is an open access repository that collects the work of Toulouse researchers and makes it freely available over the web where possible

This is an author's version published in: <http://oatao.univ-toulouse.fr/23561>

### To cite this version:

Al-Naboulsi, Tawfik  and Boulos, Madona and Tenailleau, Christophe  and Dufour, Pascal  and Zakhour, Mirvat  and Guillemet-Fritsch, Sophie *Colossal and frequency stable permittivity of barium titanate nanoceramics derived from mechanical activation and SPS sintering*. (2015) International Journal of Engineering Research & Science, 1 (7). 25-33. ISSN 1018-7375

Any correspondence concerning this service should be sent to the repository administrator: [tech-oatao@listes-diff.inp-toulouse.fr](mailto:tech-oatao@listes-diff.inp-toulouse.fr)

# Colossal and frequency stable permittivity of barium titanate nanoceramics derived from mechanical activation and SPS sintering

Tawfik Al-Naboulsi<sup>1</sup>, Madona Boulos<sup>2</sup>, Christophe Tenailleau<sup>3</sup>, Pascal Dufour<sup>4</sup>, Mirvat Zakhour<sup>5</sup>, Sophie Guillemet-Fritsch<sup>6</sup>

<sup>1,2,5</sup>Laboratoire de Chimie Physique des matériaux (LCPM, PR2N), EDST, Université Libanaise, Faculté des Sciences II, Département de chimie, Fanar, Liban

<sup>1,3,4,5</sup>Institut Carnot CIRIMAT, UMR CNRS5085. Université Paul Sabatier. 118, route de Narbonne. 31062 Toulouse Cedex 09, France

**Abstract**— *Highly dense barium titanate nanoceramics have been successfully prepared via a mechanical activation synthesis method and Spark Plasma sintering. Attractive electrical properties have been evidenced in these materials: a colossal permittivity, ( $3.5 \cdot 10^5$ ) and low loss (0.07) at room temperature and 1 kHz, that are stable over a wide frequency range (from 40 Hz to 40 kHz). Surprisingly, the ferroelectric transition is still observed, for the first time to our knowledge, in these colossal permittivity materials.*

**Keywords**— *Barium titanate, ball milling, spark plasma sintering, nanoceramics, dielectric properties.*

## I. INTRODUCTION

The ferroelectric barium titanate (BT) is one of the most studied functional materials as a free-lead ceramic thanks to its potential application as a multilayer ceramic capacitor, high- $\epsilon$  dielectric, PTC thermistor, electromechanical device, piezoelectric transducer, and dynamic RAM [1, 2].

Electrical properties of BT are highly dependent on the synthesis procedure and thermal treatments that influence the purity, structure, crystallite size, grain size... The dielectric constant increases with decreasing grain size to reach a maximum at a grain size of 1-2  $\mu\text{m}$  [3-5]. Various procedures developed to synthesize BT were reported in the literature, including coprecipitation [6, 7], hydrothermal [8, 9], sol gel [10, 11], self-propagating high-temperature synthesis [12]. Some of the mentioned synthesis methods yield to non-pure and non-homogeneous powders or require a long-time and complicated process. Ball milling can be used to synthesize nanograined powders by means of mechanical activation. It is one of the most interesting synthesis methods from an industrial point of view, since one of the less sophisticated technologies and the cheapest one. The use of ball milling activation as a top down technique can lead to nanosized powders [13-24]. Most of the ball milling procedures reported in literature require high energy (i.e. a milling speed of 4000 rpm [20], a high calcination temperature, 1000°C [23] or long reaction time 159 hours [15]).

This work aims to synthesize nanosized BT powders with a minimum energy and time. In order to keep nanosized grains in the ceramic, a field assisted sintering method, particularly the Spark Plasma Sintering (SPS), was used to consolidate the powders. It is an efficient method to produce compact nano-sized grains ceramics at low temperature and short time, which limit grain growth [25]. Previous work performed on nano BT has shown that the reductive atmosphere during sintering increases the number of charge carriers in ceramics, by the reduction of  $\text{Ti}^{4+}$  in  $\text{Ti}^{3+}$ , thus creating high concentrations of oxygen vacancies and electrons. The presence of a large number of point defects leads to colossal permittivity ( $\epsilon'$ ) [26]. If the properties of many dense nanoceramics prepared from powders issued from various synthesis methods have been reported [6, 12, 24, 26-30], very few data concern BT materials obtained from the combination of ball milling synthesis and SPS [22, 31].

Alves et al. [22] prepared dense nanostructured BT from high energy ball milling powders and evidenced a typical ferroelectric behavior, with a permittivity of  $\epsilon' = 3000$  and losses ( $\tan \delta$ ) of 3 % at 300 K and 1 kHz. Hungria et al. [31] studied the entire solid solution  $\text{Ba}_{1-x}\text{Sr}_x\text{TiO}_3$  by combining mechanosynthesis and SPS sintering. These authors found ordinary electrical properties of BT ceramics ( $\epsilon' \sim 1400$  at room temperature and 1KHz), except of a reduction of the Curie temperature to 105°C. They related this reduction to the relatively small grain size of ceramic.

The aim of this paper is to use a simple milling process with a minimum energy and time to synthesize nanometric BT powders and dense nanoceramics after low temperature SPS sintering. The structure and microstructure are carefully determined and correlated to the dielectric properties.

## II. HEADINGS

### 2.1 Sample Preparation

BaTiO<sub>3</sub> powders were prepared from powders mixture of barium carbonate (BaCO<sub>3</sub> (BC): Pro-analysis 99%), and titanium dioxide (TiO<sub>2</sub> (anatase): Acro-organic 99%) powders, that were mechanically milled at room temperature under air atmosphere in an alumina container. The choice of alumina jar was based on the results of Dang et al. [32]. The use of a jar made of steel shows an iron contamination and the appearance of a secondary phase of hexagonal perovskite structure.

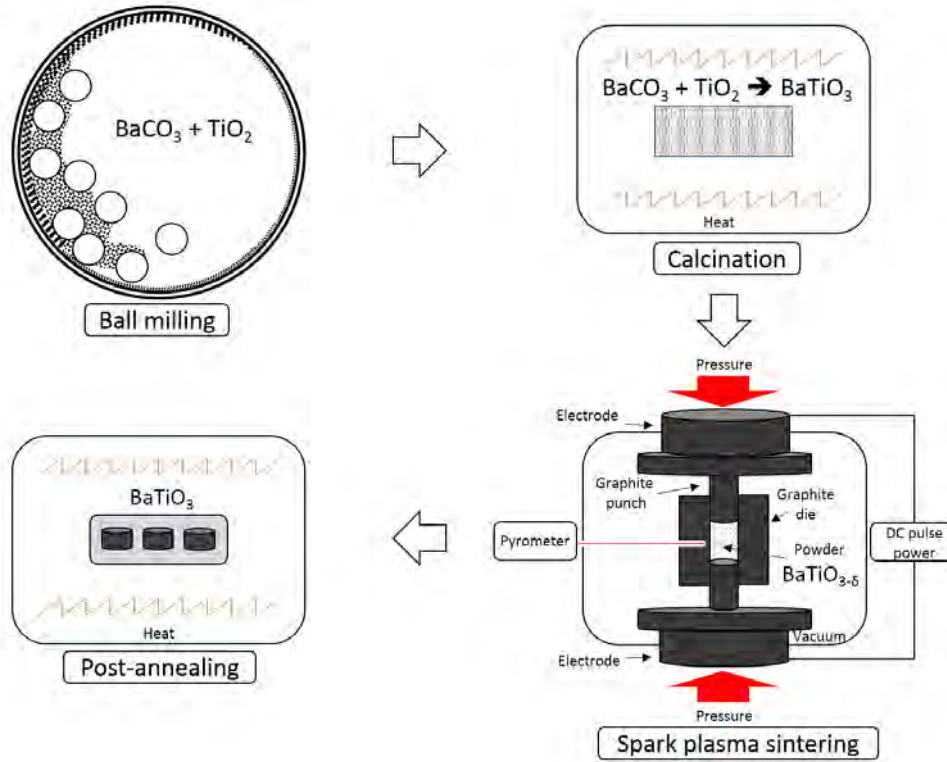


FIG 1: SCHEMA SHOWING THE CERAMICS ELABORATION PROCESS

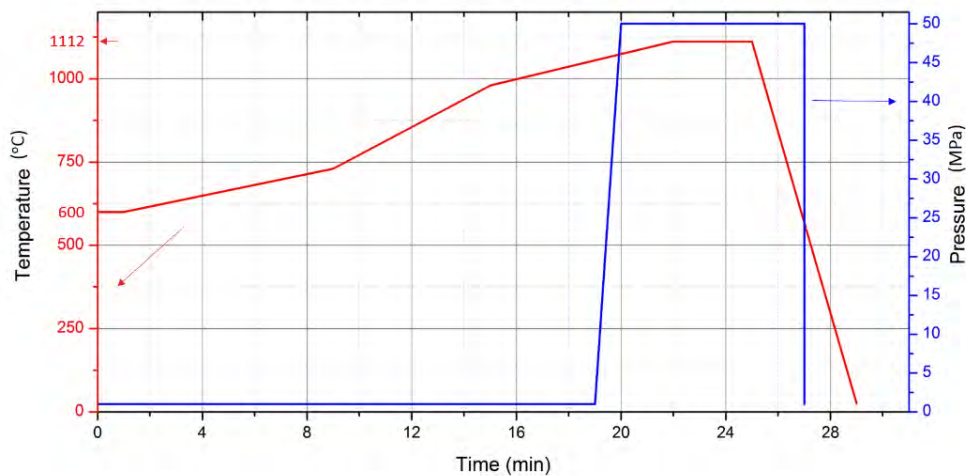


FIG 2: SPARK PLASMA-SINTERING CYCLE

The overall elaboration process of the ceramics is described in fig.1. The milling was performed during 8 hours using a Retsch PM 100 planetary apparatus at 350 rpm with a ball-to-powder weight ratio equal to 10 (Alumina balls,  $\phi = 10$  mm). The obtained powders were then heat treated in air at 900 °C for 6 hours. They were introduced without binder in an 8 mm graphite die. The die was placed in the SPS equipment (SPS Syntx Inc., Dr. Sinter 2080) for powder sintering at 1112°C during 3 min under 50 MPa (fig.2). An optical pyrometer focused on a small hole at the surface of the die was used to measure and monitor the temperature. The heating and the cooling rate were 24°C/min and 150°C/min, respectively. Finally the obtained pellets were polished to remove the graphite layers (due to graphitic contamination from the die). Sintered pellets were then post-annealed at 600°C for 15 min to perform partial re-oxidation and obtain the insulating characteristics of the ceramic samples.

## 2.2 Sample characterization

The oxide powder morphology was observed by mean of a field electron gun scanning electron Microscope (SEM-FEG, JEOL JSM 6700). The structure was identified by X-ray diffraction analysis. The data were collected on a Bruker D8 X-ray diffractometer (Cu  $K\alpha = 1.5418$  Å) from 20° to 80° (2 theta). The Raman investigation were carried out by means of Horiba xploRATM. The powder specific surface area was measured by nitrogen desorption according to the BET method (micrometrics Desorb 2300A, Flow Sorb II 2300). Assuming that the powders are constituted of single-sized and non-porous spherical particles, their geometrical surface is related to the diameter by the relation  $S = 6/(d \cdot l)$  (where S= BET specific surface area ( $\text{cm}^2 \cdot \text{g}^{-1}$ ); d = particle diameter (cm) and l = the theoretical specific mass ( $6.02 \text{ g} \cdot \text{cm}^{-3}$ ). The thermo-gravimetric analyses (TGA) were performed using a NAVAS INSTRUMENTS MMS-4000 thermo-balance. The density of the ceramics was determined by the Archimede's method. Dielectric measurements were performed on polished ceramic disks with sputtered gold electrodes on the disk faces, using an Agilent 4294A. The data were recorded in the frequency range 40 Hz - 4 MHz and in the temperature range 260K-420K.

## III. RESULTS AND DISCUSSION

TGA analysis was performed to follow the powder mass change during the calcination cycle (900°C, 6h) (Fig.3). A mass loss, corresponding to the decomposition of BC into BaO, is observed at 650 °C, a temperature which is much lower than the one reported in the literature ( $>1000$  °C) [33, 34]. It is clear that the activated powder needed less energy (temperature and time), than conventional powder, to totally decompose BC into BaO. This difference can be related to an increase in BC reactivity due to lower particle size, leading to an increase of the contact points between the precursors (BC and  $\text{TiO}_2$ ) and so to favor the mixing and interdiffusion. The experimental mass loss (15.3%) is in agreement with the theoretical one (15.9%).

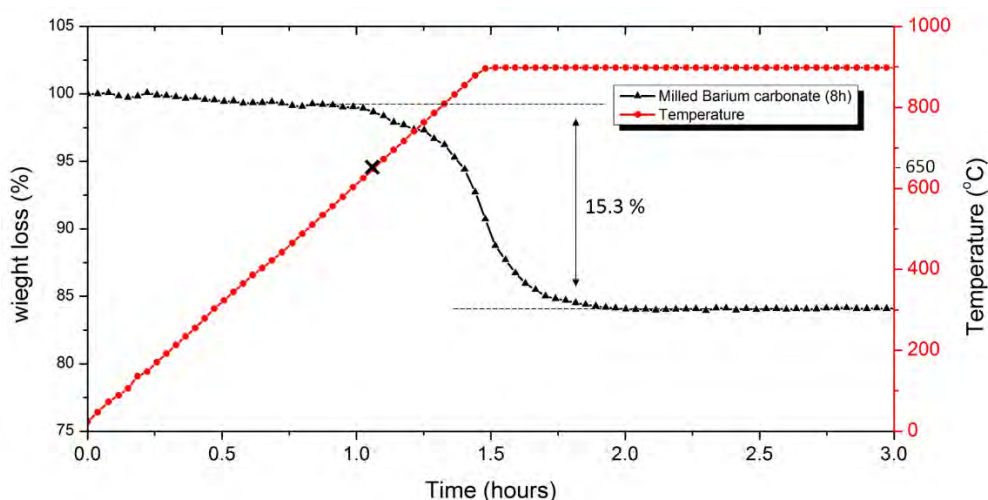


**FIG 3: TGA (IN FLOWING AIR) OF BC AND  $\text{TiO}_2$  POWDER MIXTURE MILLED DURING 8 HOURS**

XRD patterns of the commercial BC (a) and the 8h milled mixture BC and  $\text{TiO}_2$  before (b) and after calcination (c), are shown in fig.4. The powders calcined at 900°C crystallize in the cubic perovskite phase (JCPDS files 31-0174). The enlargement of the peaks observed on the XRD pattern of the milled powders (fig.4b.) can be explained by smaller crystallite size, i.e. 30-32 nm, calculated using Scherrer's equation.

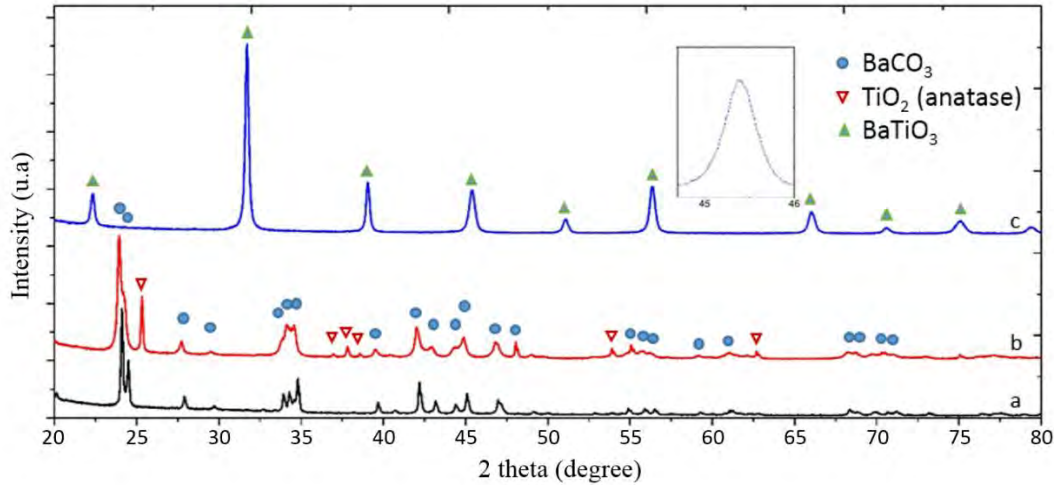


**FIG 4: XRD PATTERNS OF POWDERS: (A) COMMERCIAL BC AND THE 8H MILLED MIXTURE BC AND TiO2 BEFORE (B) AND (C) AFTER CALCINATION (FOR 6H AT 900C).**

The Raman spectrum of synthesized barium titanate powder is shown in fig.5. The spectra consists of five peaks at 185, 260, 306, 515 and 715  $\text{cm}^{-1}$ , which are all characteristic bands of the tetragonal  $\text{BaTiO}_3$  phase, which contradictory with the XRD results. This difference is completely similar to that of  $\text{BaTiO}_3$  single crystals just above Curie temperature [35, 36]. This result agrees with the Raman study of Hoshina et al. They found that below 30 nm (which is identical to our ceramic crystallites size), the average and static symmetries (from XRD measurement) were assigned to cubic, while the local and dynamic symmetries (from Raman scattering measurement) were assigned to tetragonal. Therefore, the symmetry difference below 30 nm can be originated from the intrinsic phase transition behavior of the  $\text{BaTiO}_3$  itself. [36].

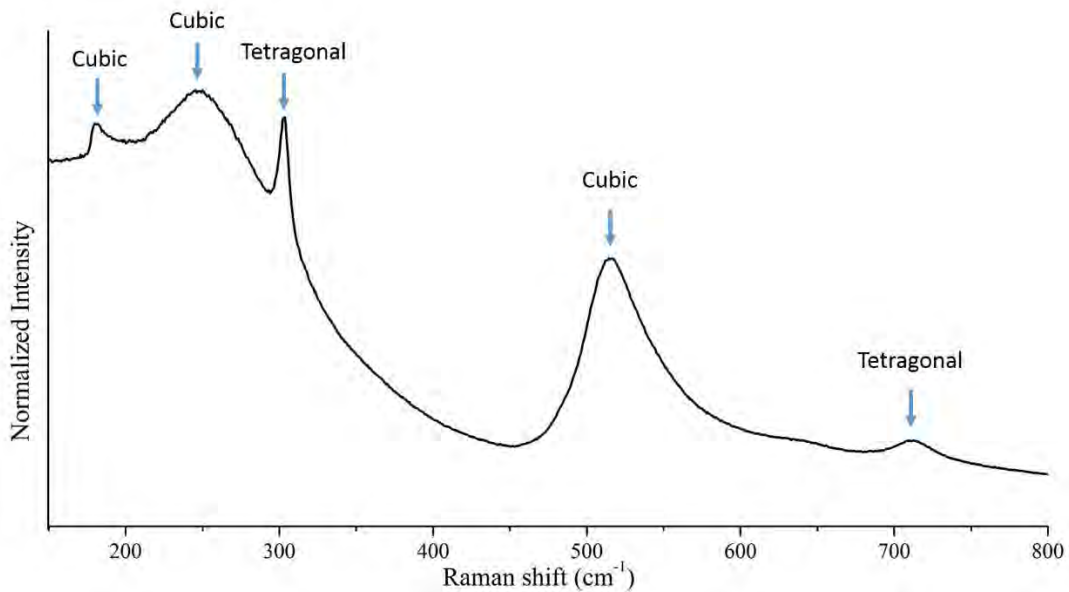


**FIG 5: RAMAN SPECTRUM OF  $\text{BaTiO}_3$  POWDERS (OBTAINED BY 8H OF MILLING AT 350 RPM, AND CALCINATED FOR 6H AT 900<sup>0</sup> C).**

Fig.6 presents the SEM-FEG images of commercial BC (a) and  $\text{TiO}_2$  (b) and the as milled mixture BC and  $\text{TiO}_2$  (c). One can notice the big difference in particle size between the pre-milled BC (0.5-3  $\mu\text{m}$ ) and the spherical nanometric  $\text{TiO}_2$  powder. In this case, 8 hours of milling were efficient to reduce the particle size of the powder mixture, down to 50-100 nm (fig.6c). The morphology and the grain size of the calcined powders are shown in fig.6d. The powders are formed by highly agglomerated spherical particles (60-80 nm), because of partial sintering during the calcination. The grain size of the agglomerates, determined from BET measurements, was approximately 220 nm (fig.6d).

After sintering, the dense pellets appeared dark blue, consistent with the presence of  $Ti^{3+}$  caused by the reducing atmosphere used during SPS (low vacuum and carbon environment). The densification is high, 98%. The ceramics crystallize in the tetragonal structure JCPDS files No. 05-0626 (fig.7), evidenced by the splitting of the (200), indicating a grain growth during sintering. Raman spectroscopy revealed also the persistence of cubic structure (not shown here).

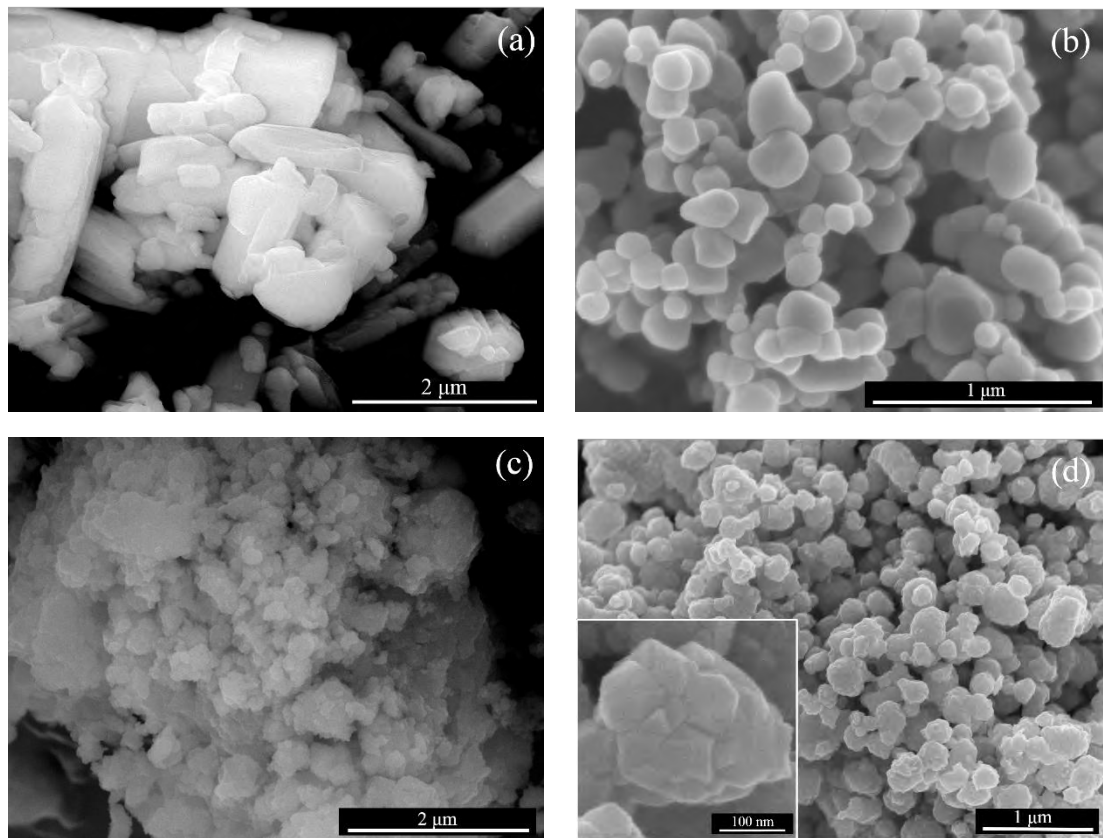


**FIG 6: SEM MICROGRAPHS OF: (A) COMMERCIAL BC AND (B)  $TiO_2$ , (C) AS MILLED MIXTURE BC AND  $TiO_2$  AND (D) BT POWDERS DERIVED FROM CALCINATION AT  $900^{\circ}C$  FOR 6H.**

SEM micrographs (Fig.8) of a cross section show few porosity, in agreement with the high densification. The grain size ranges from 400 to 900 nm.

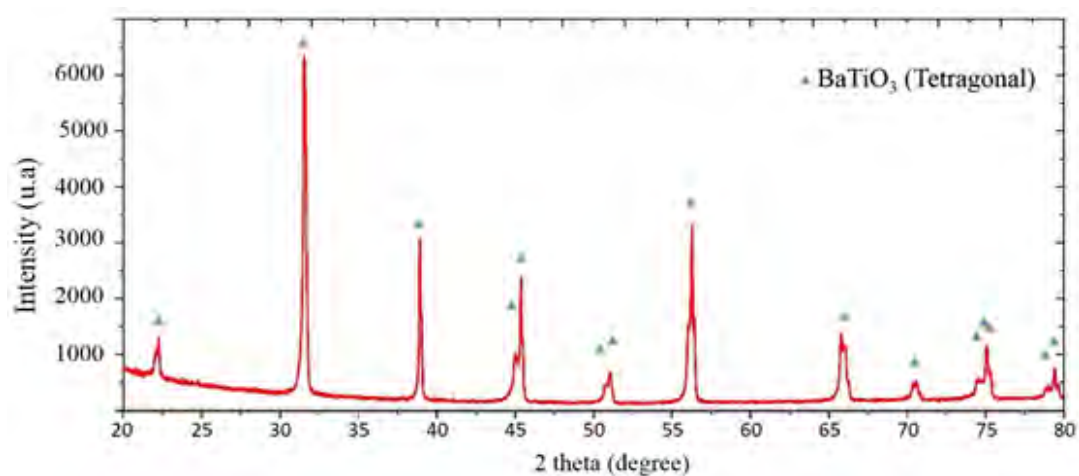


**FIG 7: XRD PATTERNS OF BT SINTERED BY SPS AT  $1112^{\circ}C$  (JCPDS No. 05-0626)**

The as sintered ceramics present a conductive behavior with high dielectric losses induced by the presence of a high number of charge carriers, due to the reduction of  $Ti^{4+}$  in  $Ti^{3+}$  during the SPS sintering. An annealing treatment is then required to obtain a capacitive behavior. Voisin et al. [37] have optimized the annealing procedure in order to keep a colossal permittivity associated with low losses. The authors explained this behavior by a core shell structure made of semi conductive grains and insulating grain boundaries, due to the presence of  $Ti^{3+}$ ,  $Ti^{4+}$  and oxygen vacancies. In our case, a temperature of 850 °C (even for a very short period of time) is too high and deteriorates the interesting properties of the nanoceramics i.e: a colossal permittivity and low dielectric losses. A lower annealing temperature was chosen, i.e. 600°C and short annealing time of 15 min, can lead to such dielectric properties. The permittivity and dielectric loss of the ceramics (post-annealed 15 min at 600°C) were measured as a function of frequency (at room temperature) and as a function of temperature (250-420 K) in a frequency range varying from 40 Hz to 1 kHz (Fig.9 a and b). At room temperature, a colossal dielectric permittivity ( $3.5 \times 10^5$ ) associated with low losses (7%) are observed. Moreover, these properties are stable in a wide frequency range (40 Hz to 100 kHz). The permittivity decreases at 100 KHz while the dielectric losses significantly increase (fig.9a).

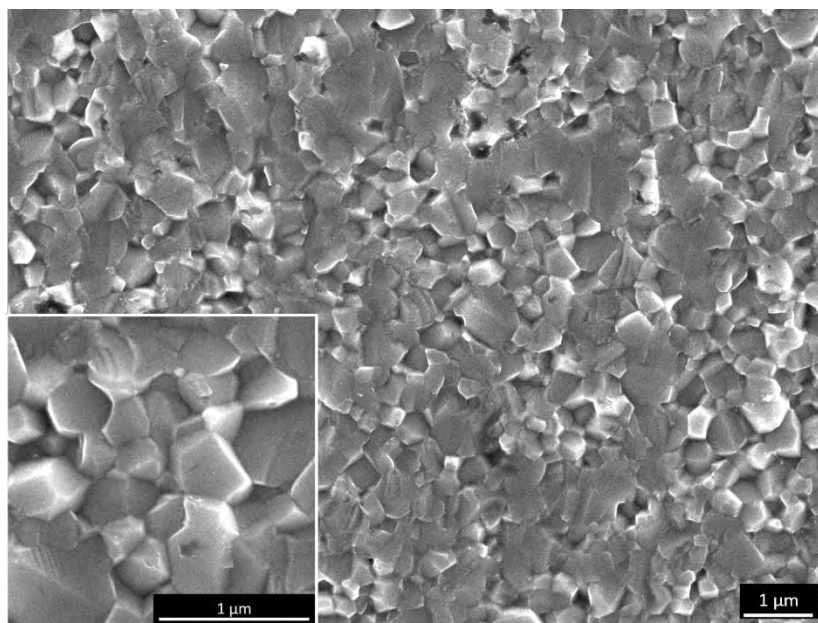


**FIG 8: SEM MICROGRAPHS OF A FRACTURE OF A BT CERAMIC**

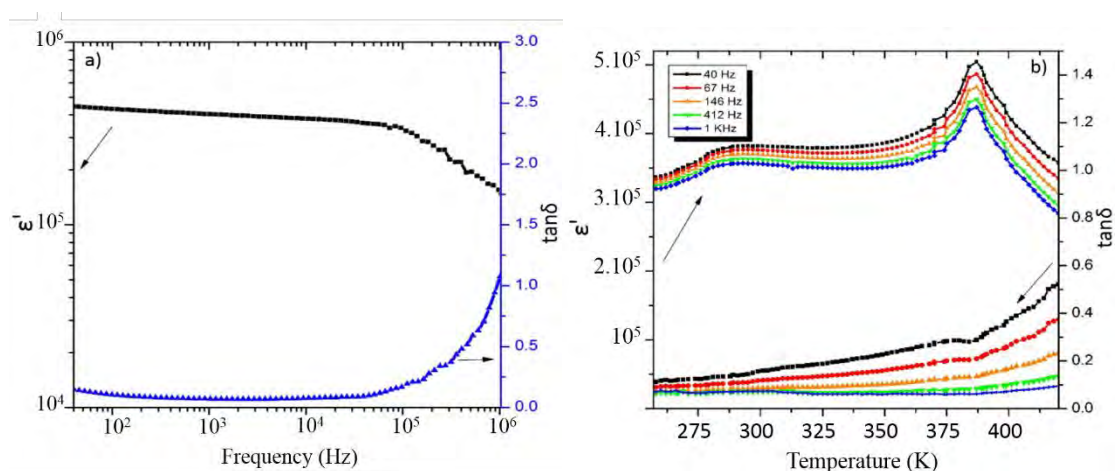


**FIG 9: A) DIELECTRIC PROPERTIES OF BT CERAMIC AS A FUNCTION OF: A) FREQUENCY (40 HZ–4 MHz) AND B) TEMPERATURE (260-420K).**

We report in Table 1 the most relevant electrical properties reported for BT nanoceramics. The high  $\epsilon'$  and low  $\tan \delta$  determined in the present work are in the same range of order of the best results obtained by Voisin et al. which were prepared by oxalate precipitation route [37]. In addition, one must retain that the colossal permittivity and the low losses are stable over a wide frequency range.

**TABLE 1: LITERATURE DATA OF BaTiO<sub>3</sub> NANOCERAMICS SYNTHESIZED BY DIFFERENT ROUTE AND SINTERED BY SPS.**

Reference	BT synthesis method	Densification	Average grain	$\epsilon'$	$\tan \delta$
Licheri et al.[12]	self-propagating high-temperature synthesis	<98%	50 nm	~ 1000	<5%
Takeuchi et al.[27]	sol-crystal method	>95%	200-400 nm	10 <sup>4</sup>	---
Luan et al.[30]	sol-gel	99%	340 -730 nm	~4000	---
Valdez-Nava et al.[6]	coprecipitation	96%	250 nm	10 <sup>5</sup>	~0.50
Sielveira et al.[24]	Ball milling	98%	500 nm	3000	~0.05
Voisin et al.[37]				5.10 <sup>5</sup>	0.05
This work		>98%	300-900 nm	3.5x10 <sup>5</sup>	~0.07

As the temperature increases (from 250-270 K) the permittivity increases and becomes independent of the temperature in the temperature range from 270 to 380K. Beyond 380K, the permittivity increases to its maximum value  $4.2 \times 10^5$  at 386K (Curie temperature) and decreases with further increase in temperature. The presence of the Curie temperature  $T_c$  (386 K), which is lower than the one usually reported, is related to the tetragonal structure. The BT structure is connected to the grains size [12, 29, 30, 38], which means that during sintering the grain size increased significantly (fig.9b). Valdez-Nava et al. have prepared by SPS (1150°C, 3min), ceramics of a pseudo-cubic structure of which the grain size is about 300 nm. In that case, these ceramics have colossal permittivity values (10<sup>5</sup>) and an absence of the Curie temperature [6]. It is the first time, to our knowledge, that nano BT still present ferroelectric transition in materials exhibiting colossal permittivity.

#### IV. CONCLUSION

Cubic structured barium titanate nanoparticles were obtained by simple ball milling of BaCO<sub>3</sub> and TiO<sub>2</sub> followed by calcination at 900°C during 6 hours. The obtained powders show a particle size of 220 nm with crystallite size of 70 nm. High density ceramics (densification >98%) were successfully obtained by SPS. The dense ceramics crystallize in the tetragonal structure, indicating grain growth during sintering. Colossal permittivity up to  $3 \cdot 10^5$  and low losses (0.07) have been evidenced at room temperature and at 1kHz. These properties are stable ( $\pm 10\%$  of variation) over a wide range of frequency (40 Hz to 40 KHz). Finally, a ferroelectric behavior is revealed in these colossal permittivity materials.

#### ACKNOWLEDGEMENTS

This work was supported by the Lebanese National Center for Scientific Research, the tow doctoral school of lebanese university (doctoral school of science and technology EDST) and Paul Sabatier III (doctoral school of material sciences SDM).

#### REFERENCES

- [1] W. Heywang, Resistivity Anomaly in Doped Barium Titanate, J. Am. Ceram. Soc., 47 (1964) 484-490.
- [2] Y. Ohara, K. Koumoto, H. Yanagida, Barium Titanate Ceramics with High Piezoelectricity Fabricated from Fibrous Particles, J. Am. Ceram. Soc., 68 (1985) C-108-C-109.
- [3] R.W.V. AZIZ S. SHAIKH, AND GERALDINE M. VEST Dielectric Properties of Ultrafine Grained BaTiO<sub>3</sub> IEEE Transactions on Ultrasonics, Ferroelectrics, and Frequency Control, 36 (1989).
- [4] K. Kinoshita, A. Yamaji, Grain- size effects on dielectric properties in barium titanate ceramics, J. Appl. Phys., 47 (1976) 371-373.



- [5] G. Arlt, D. Hennings, G. de With, Dielectric properties of fine-grained barium titanate ceramics, *J. Appl. Phys.*, 58 (1985) 1619-1625.
- [6] Z. Valdez-Nava, S. Guillemet-Fritsch, C. Tenailleau, T. Lebey, B. Durand, J.Y. Chane-Ching, Colossal dielectric permittivity of BaTiO<sub>3</sub>-based nanocrystalline ceramics sintered by spark plasma sintering, *J. Electroceram.*, 22 (2009) 238-244.
- [7] L. Wu, M.-C. Chure, K.-K. Wu, W.-C. Chang, M.-J. Yang, W.-K. Liu, M.-J. Wu, Dielectric properties of barium titanate ceramics with different materials powder size, *Ceram. Int.*, 35 (2009) 957-960.
- [8] H. Xu, L. Gao, Hydrothermal synthesis of high-purity BaTiO<sub>3</sub> powders: control of powder phase and size, sintering density, and dielectric properties, *Mater. Lett.*, 58 (2004) 1582-1586.
- [9] S.K. Lee, G.J. Choi, U.Y. Hwang, K.K. Koo, T.J. Park, Effect of molar ratio of KOH to Ti-isopropoxide on the formation of BaTiO<sub>3</sub> powders by hydrothermal method, *Mater. Lett.*, 57 (2003) 2201-2207.
- [10] R. Kaviani, A. Saidi, Sol-gel derived BaTiO<sub>3</sub> nanopowders, *J. Alloys Compd.*, 468 (2009) 528-532.
- [11] W. Li, Z. Xu, R. Chu, P. Fu, J. Hao, Structure and electrical properties of BaTiO<sub>3</sub> prepared by sol-gel process, *J. Alloys Compd.*, 482 (2009) 137-140.
- [12] R. Licheri, S. Fadda, R. Orrù, G. Cao, V. Buscaglia, Self-propagating high-temperature synthesis of barium titanate and subsequent densification by spark plasma sintering (SPS), *J. Eur. Ceram. Soc.*, 27 (2007) 2245-2253.
- [13] C. Gomez-Yañez, C. Benitez, H. Balmori-Ramirez, Mechanical activation of the synthesis reaction of BaTiO<sub>3</sub> from a mixture of BaCO<sub>3</sub> and TiO<sub>2</sub> powders, *Ceram. Int.*, 26 (2000) 271-277.
- [14] J. Xue, J. Wang, D. Wan, Nanosized Barium Titanate Powder by Mechanical Activation, *J. Am. Ceram. Soc.*, 83 (2000) 232-234.
- [15] V. Berbenni, A. Marini, G. Bruni, Effect of mechanical milling on solid state formation of BaTiO<sub>3</sub> from BaCO<sub>3</sub>-TiO<sub>2</sub> (rutile) mixtures, *Thermochim. Acta*, 374 (2001) 151-158.
- [16] H.A.M. van Hal, W.A. Groen, S. Maassen, W.C. Keur, Mechanochemical synthesis of BaTiO<sub>3</sub>, Bi<sub>0.5</sub>Na<sub>0.5</sub>TiO<sub>3</sub> and Ba<sub>2</sub>NaNb<sub>5</sub>O<sub>15</sub> dielectric ceramics, *J. Eur. Ceram. Soc.*, 21 (2001) 1689-1692.
- [17] L.B. Kong, J. Ma, H. Huang, R.F. Zhang, W.X. Que, Barium titanate derived from mechanochemically activated powders, *J. Alloys Compd.*, 337 (2002) 226-230.
- [18] M.T. Buscaglia, M. Bassoli, V. Buscaglia, R. Alessio, Solid-State Synthesis of Ultrafine BaTiO<sub>3</sub> Powders from Nanocrystalline BaCO<sub>3</sub> and TiO<sub>2</sub>, *J. Am. Ceram. Soc.*, 88 (2005) 2374-2379.
- [19] B.D. Stojanovic, A.Z. Simoes, C.O. Paiva-Santos, C. Jovalekic, V.V. Mitic, J.A. Varela, Mechanochemical synthesis of barium titanate, *J. Eur. Ceram. Soc.*, 25 (2005) 1985-1989.
- [20] S. Ohara, A. Kondo, H. Shimoda, K. Sato, H. Abe, M. Naito, Rapid mechanochemical synthesis of fine barium titanate nanoparticles, *Mater. Lett.*, 62 (2008) 2957-2959.
- [21] A.K. Nath, C. Jiten, K.C. Singh, Influence of ball milling parameters on the particle size of barium titanate nanocrystalline powders, *Physica B: Condensed Matter*, 405 (2010) 430-434.
- [22] M.F.S. Alves, R.A.M. Gotardo, L.F. Cótica, I.A. Santos, W.J. Nascimento, D. Garcia, J.A. Eiras, High density nanostructured BaTiO<sub>3</sub> ceramics obtained under extreme conditions, *Scripta Mater.*, 66 (2012) 1053-1056.
- [23] T. Sundararajan, S.B. Prabu, S.M. Vidyavathy, Combined effects of milling and calcination methods on the characteristics of nanocrystalline barium titanate, *Mater. Res. Bull.*, 47 (2012) 1448-1454.
- [24] L.G.D. Silveira, M.F.S. Alves, L.F. Cótica, R.A.M. Gotardo, W.J. Nascimento, D. Garcia, J.A. Eiras, I.A. Santos, Dielectric investigations in nanostructured tetragonal BaTiO<sub>3</sub> ceramics, *Mater. Res. Bull.*, 48 (2013) 1772-1777.
- [25] Z.A. Munir, U. Anselmi-Tamburini, M. Ohyanagi, The effect of electric field and pressure on the synthesis and consolidation of materials: A review of the spark plasma sintering method, *J. Mater. Sci.*, 41 (2006) 763-777.
- [26] S. Guillemet-Fritsch, Z. Valdez-Nava, C. Tenailleau, T. Lebey, B. Durand, J.Y. Chane-Ching, Colossal Permittivity in Ultrafine Grain Size BaTiO<sub>3-x</sub> and Ba<sub>0.95</sub>La<sub>0.05</sub>TiO<sub>3-x</sub> Materials, *Adv. Mater.*, 20 (2008) 551-555.
- [27] T. Takeuchi, Y. Suyama, D. Sinclair, H. Kageyama, Spark-plasma-sintering of fine BaTiO<sub>3</sub> powder prepared by a sol-crystal method, *J. Mater. Sci.*, 36 (2001) 2329-2334.
- [28] B. Li, X. Wang, M. Cai, L. Hao, L. Li, Densification of uniformly small-grained BaTiO<sub>3</sub> using spark-plasma-sintering, *Mater. Chem. Phys.*, 82 (2003) 173-180.
- [29] B. Li, X. Wang, L. Li, H. Zhou, X. Liu, X. Han, Y. Zhang, X. Qi, X. Deng, Dielectric properties of fine-grained BaTiO<sub>3</sub> prepared by spark-plasma-sintering, *Mater. Chem. Phys.*, 83 (2004) 23-28.
- [30] W. Luan, L. Gao, H. Kawaoka, T. Sekino, K. Niihara, Fabrication and characteristics of fine-grained BaTiO<sub>3</sub> ceramics by spark plasma sintering, *Ceram. Int.*, 30 (2004) 405-410.
- [31] T. Hungria, M. Algueró, A.B. Hungria, A. Castro, Dense, Fine-Grained Ba<sub>1-x</sub>Sr<sub>x</sub>TiO<sub>3</sub> Ceramics Prepared by the Combination of Mechanothesized Nanopowders and Spark Plasma Sintering, *Chem. Mater.*, 17 (2005) 6205-6212.
- [32] N.V. Dang, T.D. Thanh, L.V. Hong, V.D. Lam, T.-L. Phan, Structural, optical and magnetic properties of polycrystalline BaTi<sub>1-x</sub>FexO<sub>3</sub> ceramics, *J. Appl. Phys.*, 110 (2011) -.
- [33] A. Ubaldini, V. Buscaglia, C. Uliana, G. Costa, M. Ferretti, Kinetics and Mechanism of Formation of Barium Zirconate from Barium Carbonate and Zirconia Powders, *J. Am. Ceram. Soc.*, 86 (2003) 19-25.
- [34] I. Arvanitidis, D. Siche, S. Seetharaman, A study of the thermal decomposition of BaCO<sub>3</sub>, *Metallurgical and Materials Transactions B*, 27 (1996) 409-416.

- [35] S. Wada, T. Suzuki, T. Noma, M. Osada, M. Kakihana, Change of micro and macro symmetry of barium titanate single crystal around Curie temperature and its model, in: Applications of Ferroelectrics, 1998. ISAF 98. Proceedings of the Eleventh IEEE International Symposium on, 1998, pp. 487-490.
- [36] T. Hoshina, H. Kakemoto, T. Tsurumi, S. Wada, M. Yashima, Size and temperature induced phase transition behaviors of barium titanate nanoparticles, *J. Appl. Phys.*, 99 (2006) 054311.
- [37] C. Voisin, S. Guillemet-Fritsch, P. Dufour, C. Tenailleau, H. Han, J.C. Nino, Influence of Oxygen Substoichiometry on the Dielectric Properties of BaTiO<sub>3-δ</sub> Nanoceramics Obtained by Spark Plasma Sintering, *Int. J. Appl. Ceram. Technol.*, 10 (2013) E122-E133.
- [38] D.-H. Yoon, Tetragonality of barium titanate powder for a ceramic capacitor application, *Journal of Ceramic Processing Research.*, 7 (2006).